DOI: 10.1002/ejic.200600237

Controlling the Size of BaF_2 Nanocubes from 1000 to 10 nm

Peng Gao,[a] Yi Xie,*[a] and Zhen Li[a]

Keywords: BaF_2 Nanocubes / Nanostructures / Electron diffraction / X-ray diffraction

Size control of BaF_2 nanocubes has been achieved by varying reaction time and pH value, thus producing nanocubes with a controllable edge length in the range 10–1000 nm. A linear relationship between cube size and reaction time has been revealed. Furthermore, a process has been developed to separate the growing BaF_2 nanocubes from the remaining solid products at different stages of the synthesis. On the basis of the observed crystallite morphologies, we have elucidated an "extension growing" mechanism to describe the size-controlled growth of BaF_2 nanocubes using this method. Photoluminescence results demonstrate that the deoxidant selenite ions prevent the incorporation of oxygen into the BaF_2 nanocubes effectually, which will greatly affect their performance as scintillators.

Introduction

Solid inorganic fluorides have a number of uncommon properties, for example, electron-acceptor behavior, a large optical-transmission domain, high resistivity, and anionic conductivity. Inorganic nanoscale fluorides and rare-earth-doped inorganic nanoscale fluorides have attracted much interest recently because of their unique properties,[1] such as optical, electrical, and magnetic, which result from the size and shape of their particles.[2] Barium fluoride is one of the dielectric fluorides (along with CaF_2 and SrF_2) that have a wide range of potential applications in microelectronic and optoelectronic devices, such as wide-gap insulating overlayers, gate dielectrics, insulators, and buffer layers in semiconductor-on-insulator structures and more advanced 3D devices.[3] BaF_2 salts activated with rare-earth ions have also been reported to display unique luminescence properties and can be used as scintillators.[4] Recently, BaF_2 nanowires and nanocubes with arching sheet-like dendrites have been prepared in quaternary microemulsions and reverse micelles, respectively.[5] Li et al. have reported the preparation of CaF_2 nanocubes by a hydrothermal method in the absence of surfactants.[6] Monodispersed noble-metal and Cu_2O nanocubes[7] have also been synthesized by controlled oxidation–reduction reactions. However, to the best of our knowledge, there have been no reports on large-scale preparations of BaF_2 nanocubes to date. Therefore, the development of simple methods for the synthesis on a large scale is a challenge. It was reported that oxygen may be incorporated into BaF_2 as oxygen–vacancy pairs and detrimentally affect the performance of the resulting nanocubes as scintillators,[8] thus avoiding the incorporation of oxygen into the products will be necessary in industry. We have synthesized single-crystalline BaF_2 nanocubes through a simple hydrothermal precipitation procedure in the presence of selenite ions, which act as deoxidants and prevent the incorporation of oxygen effectively. The morphology and size of the final products can be manipulated through controlling the synthesis parameters such as reaction time and pH value.

Results and Discussions

Structural and Compositional Analysis

Figure 1 shows a representative XRD pattern of samples prepared with this approach, which indicates that all the products are phase-pure crystalline BaF_2 [in cubic symmetry; space group (SG) *Fm*3*m*, lattice constant *a* =

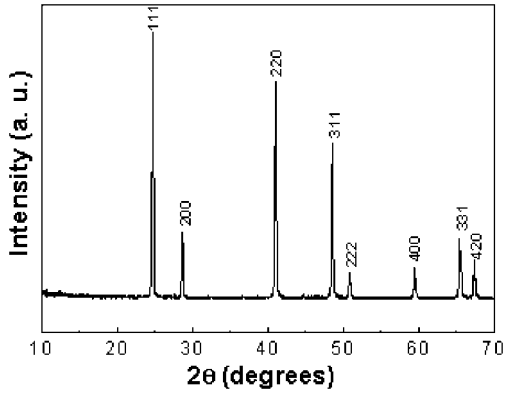

Figure 1. Powder XRD pattern of single-crystalline BaF_2 nanocubes with an edge length of 55 nm.

[a] Nano-materials and Nano-chemistry, Hefei National Laboratory for Physical Sciences at Microscale, University of Science & Technology of China,
Hefei, Anhui 230026, P. R. China
Fax: +86-551-3603987
E-mail: yxielab@ustc.edu.cn

6.19 ± 0.01 Å].[9] No other impurities have been found in the synthesized products.

Further evidence for the quality and composition of the samples was obtained by X-ray photoemission spectroscopy (XPS) of the products. An XPS measurement of the crystals shows peaks corresponding to Ba, F, O, and C (Figure 2), which agrees with results previously reported in the literature.[10] The oxygen detected in the XPS measurement may come from the atmosphere. Furthermore, low amounts of oxygen (about two percent) are frequently observed in XPS spectra. Both the results of the XRD and XPS studies leave no doubt that the product is BaF_2.

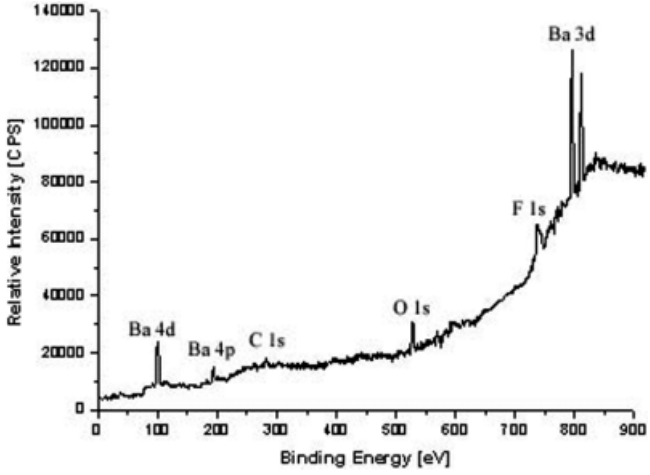

Figure 2. XPS spectrum of the BaF_2 nanocubes with an edge length of 55 nm.

Morphology of the BaF_2 Nanocubes

As shown in Figure 3a, the BaF_2 products described above have perfect cubic morphology. It is also clear that more than 95% of the BaF_2 particles have a regular cubelike structure with a mean edge length of 55 nm. The excellent crystallinity of the BaF_2 nanocubes is also confirmed by an electron diffraction (ED) experiment. Figure 3c shows a spot pattern from a single-crystalline BaF_2 nanocube (Figure 3b). In this case, the electron beam is incident along the [001] direction, and the spot array has a fourfold axis that can be indexed with *hk*0 (i.e. [001] zone spots, in accordance with the extinction rule of electron diffraction for the space group *Fm*3*m*), which indicates cubic symmetry for the BaF_2 nanocubes. Figure 3d shows a typical FESEM image of the BaF_2 nanocubes. The inset shows a FESEM image at higher magnification that clearly displays the sharp corners and edges of these nanocubes. All these observations confirm that the particles are indeed cubelike. Moreover, the nanocubes obtained from this approach are very uniform in size.

Size-Controlled Growths

In this work, size control of BaF_2 nanocubes has been achieved by varying the reaction time and adjusting the pH, and this produces BaF_2 nanocubes with a controllable edge length in the range 10–1000 nm.

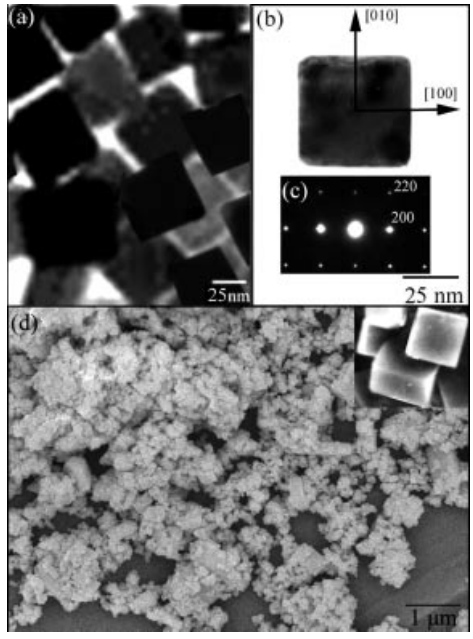

Figure 3. (a) TEM image of the BaF_2 nanocubes (pH = 2, 0.002 mol SeO_2 for 24 h). (b) TEM image of one BaF_2 single-crystalline nanocube. (c) Electron diffraction pattern of the nanocube in (b). (d) Typical FESEM images of the as-synthesized BaF_2 nanocubes. The inset shows a magnified FESEM image that illustrates the sharp corners and edges of these nanocubes.

With a simple variation in the reaction time (or ageing time), the size of these nanocubes can be controlled easily. In fact, we have obtained nanocubes as small as 10 nm (average edge length) with an ageing time of 3 h, as reported in Figure 4 and Figure 5a. After a reaction time of only 3 h, these BaF_2 nanoparticles started to show cubic type morphology, although they are not as well-faceted as samples obtained with longer ageing times. In principle, it is possible to capture even smaller particles by drawing samples at ageing times shorter than 3 h. However, the extremely low yield makes it impractical to do so. Nonetheless, the possibility of synthesizing even smaller (a few nanometers) and yet uniform nanocubic BaF_2 is positively indicated. With ageing times of 12 and 24 h (as shown in

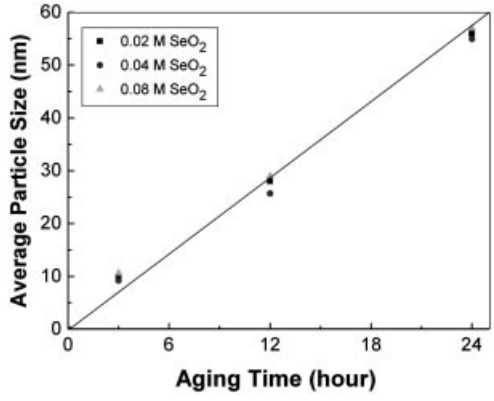

Figure 4. Average size of BaF_2 nanocube edges as a function of ageing time and SeO_2 added. The line is linearly fitted with R^2 = 0.98.

Figure 5b and Figure 3a, respectively), the particles gradually increase in size and are better faceted. As can be seen in Figure 4, the size kinetics appears to be linear with respect to time and independent of the amount of SeO_2 added under the synthesis conditions investigated (i.e. 0.02 M of SeO_2 was sufficient to generate the cubelike morphology). On the basis of the TEM image statistics, it is found that the amount of SeO_2 used (either 0.02 or 0.08 M) does not have a substantial influence on the sizes of the nanoparticles. Although our primary focus in this work is on BaF_2 nanocubes in the range 10–50 nm, this linear relationship is likely to extend further. TEM image statistics also indicate an improvement in size uniformity for the long-aged samples.

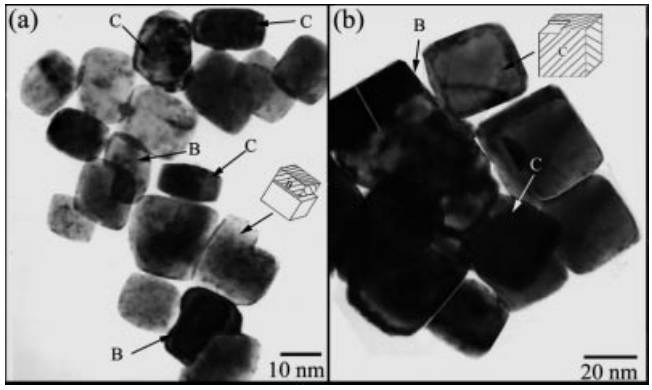

Figure 5. TEM images of BaF_2 nanocubes prepared (0.04 M SeO_2, pH = 2) with ageing times of: (a) 3 h and (b) 12 h (crystallite types B and C have been marked).

Varying the pH value of the system, while keeping other synthesis parameters unchanged, leads to a dramatic change in the size and shape of the particles. Figure 6 and Table 1 show the morphologies and sizes of the particles obtained by increasing the pH value of the system. It is found that when the pH value is small (≈2), the nanoparticles are smaller, and their shapes are cubic; When pH value ≥ 2, only larger nanocubes form; in the pH value range 2–6, a clear transition from small cubic particles is observed. Only octahedral particles with a mean edge length of 1 μm form when the pH value is raised to 7.

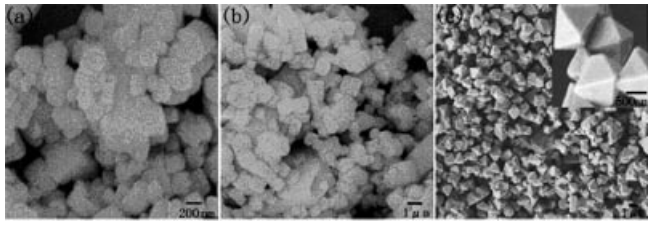

Figure 6. FESEM images of BaF_2 nanoparticles prepared (0.04 M SeO_2, ageing time 24 h) with different pH values: (a) pH = 4, (b) pH = 6 and (c) pH = 7.

Table 1. The morphologies and mean sizes of BaF_2 nanoparticles at different pH values.

pH value	Morphology	Mean size [nm]
2	Cube	55
4	Cube	200
6	Cube	1000
7	Octahedron	1000

Growth Mechanism

In Figure 5, a considerable amount of BaF_2 nanoparticles (marked with arrows) show special morphologies, although the majority of the BaF_2 crystallites are highly symmetrical nanocubes with equal edges. Aside from the normal, perfect nanocubes (type A), there are two types of "abnormally grown" nanocubes. As illustrated further in Scheme 1, the first one, type B, indicates some sidewall extension. The second one, type C, results largely from an in-plane completing growth. All crystallites observed can be broadly classified as either type A, type B, or type C, a finding also reported for Co_3O_4 nanocubes.[11] As depicted in the literature, a correct sequential arrangement of these crystallite types would naturally disclose the nanocube growth mechanism, a logical repetition of the three types of nanocrystallites, i.e. $\cdots\rightarrow A_{smaller} \rightarrow B \rightarrow C \rightarrow A_{larger} \rightarrow\cdots$. Thus, the growth does not proceed in a layer-by-layer manner (atomically), but with multiple-layer growth, i.e. nucleation and growth take place simultaneously in different atomic layers.

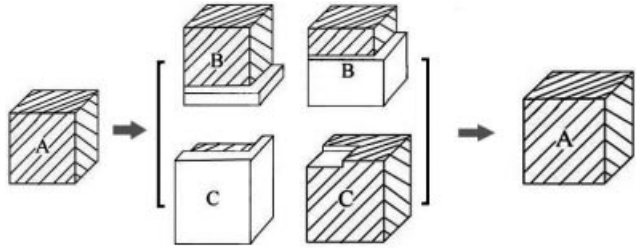

Scheme 1. Schematic illustration of the "extension growing" process based on the morphologies of intermediate crystallites (B and C) observed. The crystallite types B and Chave also been referred to in Figure 5.

In this approach, SeO_2 plays a critical role in the formation of the BaF_2 nanocubes. Firstly it acts as deoxidant, to prevent the incorporation of oxygen, which will affect the luminescence properties of BaF_2.[8] Photoluminescence experiments were carried out at room temperature on a Perkin–Elmer Model LS-55 fluorescence spectrometer with a Xe lamp. Photoluminescence results, as shown in Figure 7, display a weak emission peak at 453 nm (2.74 eV), which is excited at 270 nm (4.59 eV). The luminescence band at 2.74 eV results from an oxygen–vacancy complex with an oxygen on a fluorine site with a next-nearest fluorine vacancy on the surface of the nanocrystals.[12] It is believed that the deoxidant selenite ions prevent the incorporation of oxygen into BaF_2 effectively during the growth process, as the emission peak is so weak that it is difficult to be detected. Under the same conditions, the PL spectrum of BaF_2 with oxygen incorporated displays an intense peak

$$(SeO_2)_{bulk} + H_2O \Leftrightarrow H_2SeO_3 \Leftrightarrow 2H^+ + SeO_3^{2-} \Leftrightarrow H_2SeO_3 \Leftrightarrow (SeO_2)_{small\ crystal} + H_2O$$
$$+ \qquad +$$
$$2F^- + Ba^{2+} \Leftrightarrow BaF_2$$
$$\Updownarrow \qquad \Updownarrow$$
$$2HF \qquad BaSeO_3$$

Scheme 2.

(several hundred times that of BaF_2 prepared by using SeO_2) at the same position. The trace oxygen may come from the atmosphere when the products were examined. Secondly, it is believed that SeO_2 which is tetragonal in symmetry (a = 8.3 Å, c = 5.1 Å) acts as a seed for the growth of the BaF_2 nanocubes. The [001]-oriented BaF_2 has a fourfold-symmetric a plane with a = 6.2 Å, which matches well to the fourfold-symmetric SeO_2 (001) substrate, $4a_{BaF_2} \approx 3a_{SeO_2}$, and this results in a c-axis-oriented growth of BaF_2 on SeO_2 (001). A small quantity of crystalline SeO_2 was also found in the sample prior to washing with distilled water and anhydrous alcohol. In this solution system, SeO_2 undergoes a recrystallization process, which is illustrated in Scheme 2.

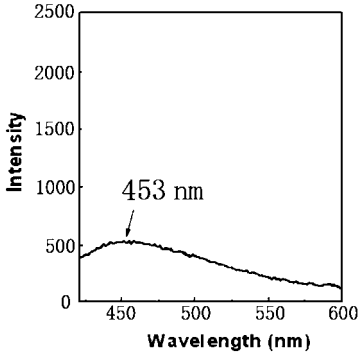

Figure 7. Photoluminescence (PL) spectra acquired from the 55-nm BaF_2 nanocubes excited at 270 nm.

When the pH value is lowered, more crystalline SeO_2 seeds form, which provides more nucleation points for the BaF_2 nanoparticles. This prevents the nanoparticles from aggregating and leads to the formation of smaller nanocubes, as illustrated in Table 1. When the pH value is increased to 7, only octahedral crystals are obtained. This is considered to be related to the enhanced surface energy of the BaF_2 nanooctahedra in the absence of SeO_2 seeds, which leads to more stable {111} faces being exposed. These results also indicate that the growth rate along <100> relative to that along <111> can be manipulated by adjusting the pH value, which will dictate whether nanocubes or nanooctahedra are formed. The concentration of SeO_2 (either 0.02 or 0.08 M) does not have a substantial influence on nanoparticle size (Figure 4) probably because at either of these concentrations, the solution is already saturated with small crystalline seeds of SeO_2. No $BaSeO_3$ is found in the product as a result of the acidic conditions.

Conclusions

In summary, by controlling the reaction time and pH values, BaF_2 nanocubes of different sizes have been prepared in the range 10–1000 nm with high crystallite-monodispersity. The relationship between the size of the cube and reaction time is found to be linear. Furthermore, on the basis of the observed crystallite morphologies, an "extension growing" growth mechanism has been elucidated for the formation of the BaF_2 nanocubes. The growth of the BaF_2 nanocubes proceeds in a multiple-layer manner. This work may uncover new ways for preparing other nano-polyhedra.

Experimental Section

Preparation of BaF_2 Nanocubes: In a typical growth procedure for BaF_2 nanocubes, $BaCl_2$ (0.002 mol), SeO_2 (0.002 mol), and NaF (0.004 mol) powders were combined in distilled water (30 mL) and stirred for 2 min. The solution pH was then adjusted with hydrochloric acid solution until its pH value was about 2. The sample (about 50 mL) was placed in a 60 mL autoclave with a Teflon liner, which was maintained at 140 °C for 24 h and then air cooled to room temperature. After reaction, the white precipitate was collected and washed thoroughly with distilled water and anhydrous alcohol. The product was dried in a vacuum at 50 °C for 4 h.

Sample Characterization: The samples were characterized by X-ray powder diffraction using a Rigaku D/max-Rapid X-ray diffractometer equipped with a copper anticathode and secondary graphite monochromator (Cu–$K_{\alpha 1,2}$, λ = 1.54178 Å). A scan rate of 0.05°/s was used to record the patterns in the 2θ range 20–70°. TEM images and ED patterns were taken on a Hitachi Model H-800 instrument with a tungsten filament, with an accelerating voltage of 200 kV. The FESEM image was obtained with a JSM-6700F field emission scanning electron microanalyser (JEOL, Japan), where the resulting powders were mounted on a copper slice. X-ray photoelectron spectroscopy (XPS) was performed with an ESCALab MKII X-ray photoelectron spectrometer, using Mg-K_α X-ray radiation as the excitation source. The binding energies obtained in the XPS analysis were calibrated against the C 1s peak at 284.2 eV.

Acknowledgments

Financial support from the National Natural Science Foundation of China and the Chinese Academy of Sciences is gratefully acknowledged.

[1] a) C. M. Bender, J. M. Burlitch, D. Barber, C. Pollock, *Chem. Mater.* **2000**, *12*, 1969–1976; b) H. Lian, M. Zhang, J. Liu, Z. Ye, J. Yan, C. Shi, *Chem. Phys. Lett.* **2004**, *395*, 362–365; c)

R. N. Hua, C. Y. Zang, C. Sha, D. M. Xie, C. S. Shi, *Nanotechnology* **2003**, *14*, 588–591.
[2] a) J. A. Creighton, D. G. Eadon, *J. Chem. Soc., Faraday Trans.* **1991**, *87*, 3881–3891; b) Y. W. Cao, R. Jin, C. A. Mirkin, *J. Am. Chem. Soc.* **2001**, *123*, 7961–7962.
[3] R. Singh, S. Sinha, P. Chou, N. J. Hsu, F. Radpour, *J. Appl. Phys.* **1989**, *66*, 6179–6185.
[4] A. J. Wojtowicz, *Nucl. Instrum. Methods Phys. Res., Sect. A* **2002**, *486*, 201–207.
[5] a) M. H. Cao, C. W. Hu, E. B. Wang, *J. Am. Chem. Soc.* **2003**, *125*, 11196–11197; b) H. Z. Lian, Z. R. Ye, C. S. Shi, *Nanotechnology* **2004**, *15*, 1455–1458.
[6] X. M. Sun, Y. D. Li, *Chem. Commun.* **2003**, 1768–1769.
[7] a) Y. G. Sun, Y. N. Xia, *Science* **2002**, *298*, 2176–2179; b) L. F. Gou, C. J. Murphy, *Nano Lett.* **2003**, *3*, 231–234.
[8] a) J. M. Vail, E. Emberly, T. Lu, M. Gu, R. Pandey, *Phys. Rev. B* **1998**, *57*, 764–772; b) E. Radzhabov, P. Figura, *Phys. Status Solidi B* **1994**, *186*, 37–40.
[9] Joint Committee on Powder Diffraction Standards (JCPDS), file no. 4-452.
[10] L. H. Lu, H. N. Cui, W. Li, H. J. Zhang, S. Q. Xi, *Chem. Mater.* **2001**, *13*, 325–328.
[11] J. Feng, H. C. Zeng, *Chem. Mater.* **2003**, *15*, 2829–2835.
[12] U. Rogulis, S. Schweizer, J. M. Spaeth, *J. Phys.: Condens. Matter* **2002**, *14*, 6949–6956.

Received: March 16, 2006
Published Online: June 23, 2006

